Modelling of the long-term behaviour of transition zones
Prediction of track settlement

Wang, Haoyu; Markine, Valeri

DOI
10.1016/j.engstruct.2017.11.038

Publication date
2018

Document Version
Accepted author manuscript

Published in
Engineering Structures

Modelling of the long-term behaviour of transition zones: Prediction of track settlement

Haoyu Wang, Valeri Markine
Delft University of Technology, Delft, the Netherlands

Abstract

Transition zones in railway tracks are the locations with considerable changes in the vertical support structures. Typically, they are located near engineering structures, such as bridges, culverts, tunnels and level crossings. In such locations, the variation of the vertical stiffness and the differential settlement of the track (when the foundation settles unevenly) result in amplification of the dynamic forces acting on the track. This amplification contributes to the degradation process of ballast and subgrade, ultimately resulting in the deterioration of vertical track geometry (settlement).

To analyse and predict the accumulated settlement of the track in transition zones, a methodology using the iterative procedure is proposed. The methodology includes the finite element simulations of the vehicle-track and sleeper-ballast interaction during a train passing a transition zone; and iterative calculations of accumulated track settlement, based on an empirical model for ballast settlement.

The simulations are performed using a 3-D dynamic finite element model (explicit integration) of a track transition zone, which accounts for the differential stiffness and the differential settlement of the track. Also, nonlinear contact elements between sleepers and ballast are used. As a result, the model can perform the detailed analysis of the stresses in ballast and accounts for the effects of vehicle dynamics. The model was validated against field measurements. The empirical settlement model describes the two-stage settlement of ballast and the nonlinear relationship between ballast stresses and permanent settlement.

The proposed methodology is demonstrated by calculating the track settlement in the transition zone for 60,000 loading cycles (3.5 MGT). The dynamic responses such as ballast stresses are analysed to study the effect of the settlement. The parametric study of the iteration step used in the accumulated settlement procedure has been performed, based on which the optimal step is suggested.

Keywords: Railway track modelling, Transition zone, Empirical settlement model, Settlement prediction.

1 Introduction

Transition zones in railway tracks are locations with considerable changes of the vertical support structures. Typically, they are located near engineering structures, such as bridges, culverts, tunnels, and level crossings. In such locations, the variation of the vertical stiffness and the differential settlement of the track (when the foundation settles unevenly) result in amplification of the dynamic forces acting on the track. This amplification contributes to the degradation process of ballast and subgrade, ultimately resulting in the deterioration of the vertical track geometry (settlement), which typically manifests itself in a 'dip' in the vertical geometry profile of the track. An example of a track deflection profile obtained by the measurement train in a transition zone is shown in Figure 1. Figure 1 shows the signature of the track deformation under the passage of Eurailscout UFM120 [1]. This deformation signature was derived from the measured acceleration signature using a double integration method. Figure 1 identifies the embankment and bridge lengths.

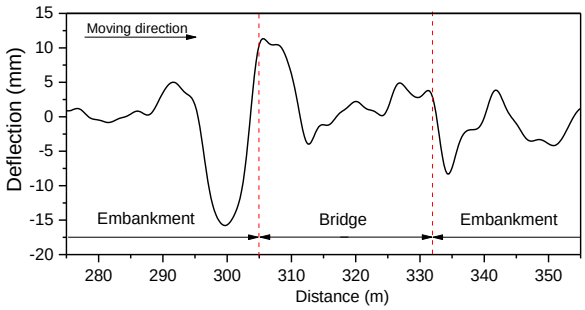

Figure 1: Measured track deflection profile in a track transition zone in the Netherlands by EurailScout.

The track profile in Figure 1 shows that two significant deflections appear before and after the bridge, indicating that the track suffers from extra settlements. Such dips are often reported in the literature [2-6]. According to a survey of nine railway companies in the US, approximately half of all railway bridges were affected by dips [7]. Such a significant irregularity in the track geometry may trigger considerable wheel-rail interaction forces, which may result in extensive damage to track components, affect passenger's comfort, and lead to even larger permanent settlements. Ultimately, it may raise the need for additional maintenance and hence increase the life cycle costs of tracks. For example, the maintenance activities on the track in transition zones are performed 4-8 times more often than that on the open tracks in the Netherlands [8, 9].

The dynamic behaviour of transition zones including level crossings has already been studied, in [2, 6, 10-32]. In these studies, the short-term behaviour (i.e. behaviour due to a single passage of a train) of track in transition zones was analysed. However, in an exhaustive review of transition zones [32], Sañudo et al. indicated that the studies on the long-term behaviour of the track in transition zones are somewhat lacking. Except in [10, 33], the settlement in transitions was predicted using 2D beam-spring track models combining with empirical models.

This paper presents a methodology to predict the accumulated settlement of the track in transition zones. The methodology combines a 3D FE (finite element) model of the transition zone and an empirical model for ballast settlement. The FE model has several novel features to thoroughly consider the nonlinearity of the sleeper-ballast contact (surface to surface contact [34],

further explained in Section 3.1) as compared to the existing models. In addition, an iterative procedure is used to predict the settlement in transition zones, wherein the transition zone model is coupled with the ballast settlement model based on the relationship between ballast stress and settlement [35]. In addition, the parametric study of the prediction procedure is performed.

In comparison to the existing methodologies, the proposed methodology can predict more precisely the settlement of transition zones, albeit the process would be computationally more expensive. The highlights of the methodology are as following:

- Behaviour of hanging sleepers in transition zones is more accurately described, since contact elements are used to model the interface between sleepers and ballast;
- More realistic settlement curve of rails and the hanging distance of sleepers can be obtained, using pre-loading step in the explicit FE analysis;
- The stresses in ballast and the effects of vehicle dynamics can be calculated;
- The nonlinear relationship between ballast stresses and settlement is considered in the settlement model.

The methodology provides a basis to study the growth of ballast settlement and the geometry degradation of tracks in transition zones. Also, the dynamic responses due to the ballast degradation can be analysed. The methodology can also be used for the comparative analysis of various transition designs. The methodology was originally presented in [36]. The main parts of the procedure are:

(I) simulation of the vehicle-track and sleeper-ballast interaction during a train passing the transition zone, using the 3-D FE transition zone model, to obtain the stresses in the ballast;

(II) calculation of the track settlement for a given number of loading cycles based on the ballast stresses, using the empirical settlement model;

(III) adjusting the FE transition zone model based on the calculated settlement under each sleeper for the step (I) in the next iteration.

The paper is organised as follows. The studies on track settlement are reviewed in Section 2. The FE transition zone model, the empirical settlement model of ballast track, and the integration of models are described in Section 3. In Section 4, the iteration scheme is demonstrated by calculating the track settlement in the transition zone for 60,000 loading cycles, or 3.5 MGT (Million Gross Tonnes). Also, the dynamic responses such as the ballast stress at 0 and 60,000 cycles (3.5 MGT) are compared to study the effect of settlement. In addition, the parametric study of the iteration step is performed. Finally, conclusions are drawn in Section 5.

2 Theory of settlement in transition zones

In [3], the average track settlements on open tracks, approaching zones and bridges were measured on several transition zones, as shown in Figure 2. The settlement is accumulated within one maintenance interval, which was 80 MGT of traffic. This figure shows that the settlement on the open track is higher than that on the bridge, and the settlement on the approaching zone is higher than that on the open track. It should be noted that the tracks on bridges in this study are ballast track; therefore the settlement of tracks on bridges is not zero. These findings in Figure 2 are in agreement with the deflection of the track shown in Figure 1.

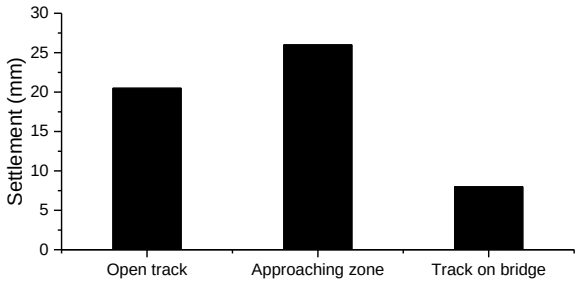

Figure 2: Comparison of the settlement in different locations of the transition zones, plotted according to [3].

The high settlement appearing in transition zones usually results from the following three aspects:

(I) the differential settlement between ballast tracks and engineering structures, which can also be considered as the geometrical irregularity, playing a major role in the degradation process of transition zones [4, 18, 19, 37-39];

(II) the significant abrupt change in the vertical stiffness of tracks;

(III) geotechnical, construction and maintenance issues [3, 7].

Note that both factor (I) and (II) lead to the increase of wheel loads, which in turn increases track settlement [2, 10]. The higher settlement of ballast tracks as compared to that of engineering structures is mainly due to the breakage and pulverisation of ballast, compaction of ballast and soil layer, and soil-water response [40]. After construction or tamping of open tracks, the permanent settlement of ballast can be divided into two stages, according to the deformation mechanism of ballast [41-44], as schematically shown (the solid line) in Figure 3. Stage 1 is the rapid compaction and abrasion process that happens within 3 to 6 months [41, 42]. In this stage, the main deformation mechanism is the volumetric compaction of particles. Stage 2 is the normal settlement process happening until the end of a maintenance interval, wherein the main deformation mechanism is the frictional sliding of particles [41, 45-48]. The settlement growth for open tracks is nonlinear in stage 1, while that is almost linear in Stage 2 [41, 43].

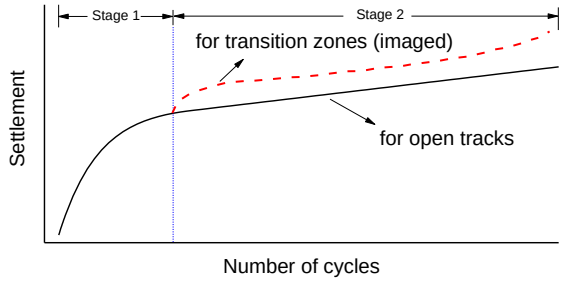

Figure 3: Schematic settlement curve of ballast as a function of loading cycles. Solid line: settlement in open tracks; dash line: the imaged settlement in transition zones.

Since the tracks on engineering structures are settled much less as compared to (open) ballast tracks, differential settlement can be generated. According to the numerical simulations presented in [37, 39], the dynamic responses such as wheel-rail interaction forces, sleeper accelerations, ballast stresses, and rail stresses are increased due to the presence of differential settlement. For example, the introduction of 2mm differential settlement triggers 100% growth of the interaction force as compared to the perfect geometry [39]. Due to the differential settlements, the ballast in transition

zones degrades at a higher rate, as the schematic curve (the dashed line) shown in Figure 3. The track degradation eventually generates dips. It should be noted that the settlement curve of the ballast in transition zones is the purpose of this study.

The degradation process of track transition zones is schematically shown in Figure 4. The effect of the stiffness variation between the embankment and the engineering structure is ignored in this figure, since its contribution is relatively small [37, 39].

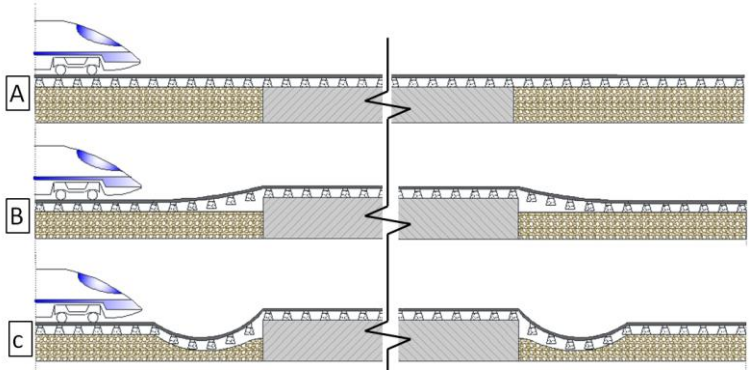

Figure 4: The process of degradation of transition zones.

Figure 4(a) shows the track with the perfect geometry before operation (right after construction). After few months of operation, the ballast track settles with a uniform value, which creates the void under sleepers near the bridge (hanging sleepers), shown in Figure 4(b). Here assuming the settlement of the engineering structure is negligible. Dips appear on both transition zones (approaching and exiting regions of the bridge) and it is remarkable that the geometries of the dips on two sides differ due to the difference in the track–vehicle dynamic interaction in these local zones.

To predict the settlement of tracks in the long term, it is common to combine the numerical vehicle-track interaction models and the empirical settlement models [49]. The dynamic responses calculated by numerical models are used as input to empirical settlement models to predict the settlement after a number of loading cycles. The empirical settlement models are mainly obtained using measurements, considering various factors including number of cycles, tonnage, ballast property, soil contamination, sleeper pressure, ballast acceleration, sleeper type, load history, the velocity of load, the variation of load (i.e. if they do not have the same amplitude), and the frequency of load [33, 50, 51]. An exhaustive review of the empirical settlement models for open tracks can be found in [43]. The empirical settlement model of ballast proposed by Sato [35] is commonly used, e.g. in [48, 49].

By using the models for calculation of the settlement separately under each sleeper, the track settlement of special structures can be predicted. In [49], Li et al. used the combination of the software GENSYS, NASTRAN (an FE software) and an empirical settlement model to predict the settlement in turnout zones. In [52], Fröhling combined a dynamic vehicle-track model with an empirical settlement model to predict the settlement due to vertical irregularities and variation of track stiffness in a section of ballast track. In [53], Suzuki et al. used the combination of a dynamic vehicle-track model (beam, mass and spring system) and an empirical settlement model to predict the settlement at rail joints. In [48], Iwnicki et al. used a combination of the simulation software MEDYNA and ADAMS/Rail (a multibody software) and empirical settlement models to predict the settlement of open tracks. In [54],

Holtzendorff and Gerstberger employed a similar method to predict the settlement of the open tracks with the quasi-periodic void pattern.

In this study, the developed FE model of transition zones using LS-Dyna and the empirical settlement model are combined to predict the long-term track behaviour in transition zones. The transition zone consists of two ballast tracks and a short bridge, which is widely used in the Netherlands. Because the initial settlement stage of rapid compaction (Stage 1 in Figure 3) of ballast track is relatively short and mainly determined by the compaction of the ballast bed, it is considered as a given value. The methodology predicts the settlement in the second stage (Stage 2 in Figure 3). It should be noted that only the settlement of ballast is considered since ballast contributes the most to the settlement of tracks [6, 42] and the computation power is limited at the current stage.

3 Methodology for settlement prediction

In this section, the methodology for the prediction of the track settlement in transition zones is presented. The methodology combines the FE model of transition zones and a settlement model of ballast. The transition zone model is briefly described below.

3.1 Finite element model of transition zones

The FE model of transition zones consists of two ballast tracks and one track on the bridge in the middle, which is modelled according to a widely used transition zone in the Netherlands, as shown in Figure 5. The railway vehicle moves from one ballast track to the other, passing the bridge. Thus, using this model, it is possible to compare the two travel directions of trains, which are named as embankment-bridge and bridge-embankment in the paper.

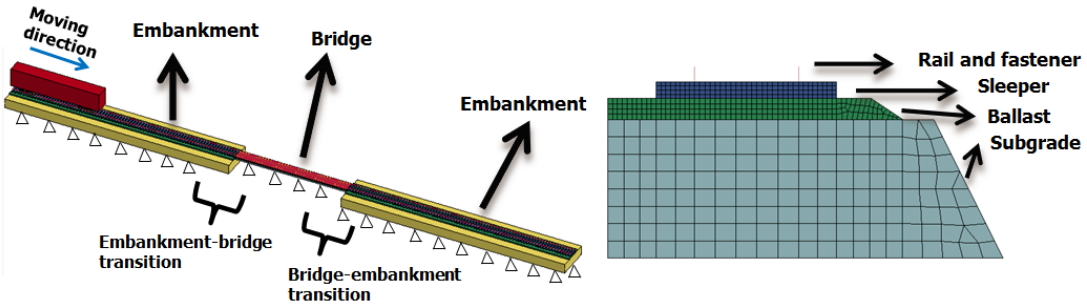

Figure 5: FE model of track transition zones.

The length of ballast track is 48m (on both sides of the bridge), and the bridge is 24m. Therefore the total length of the model is 120m (48+24+48=120). The components of the ballast tracks are rails, fasteners, sleepers, ballast and subgrade. The rails are modelled by Hughes-Liu beam elements with 2*2 Gauss quadrature integration [34], whereas the cross-sectional and mass properties of the UIC54 rail are used. The spring and damper elements between rails and sleepers are used to model fasteners. In the vertical direction, these springs have bilinear properties. Thereby, in compression they have the stiffness of rail pads; and in tension the stiffness is much higher to simulate the clamping effect of the fasteners. The tension stiffness is assumed as 1000 times of the compression stiffness. Ballast, sleepers and subgrade are modelled using the fully integrated solid elements with elastic material properties. The thickness of ballast and subgrade is 0.3m and 2m, respectively. The material properties of the elements used in the model are collected in Table 1 and Table 2.

Table 1: Material properties of solid elements.

	Elastic Modulus (MPa)	Poisson ratio

Sleeper	3650	0.167
ballast	120	0.250
Subgrade	180	0.250
Concrete bridge slab	3500	0.167

Table 2: Material properties of fasteners.

	Horizontal	Vertical	Longitudinal
Stiffness (KN/mm)	1.5	120 (compression) 120 000 (tension)	1.5
Damping (N·s/m)	5000	5000	5000

The vehicle is a passenger train, which is idealized as a multibody system. It consists of a car body, two bogies and four wheelsets connected by the primary and secondary suspensions, which are modelled using rigid bodies and spring-damper elements. The velocity of the train is 200km/h. The configurations and the parameters of the train are shown in Table 3.

Table 3: Vehicle parameters.

Parameter	Value	Parameter	Value
Axle load (kN)	142	Primary suspension stiffness (N/m)	8.80e5
Distance between wheels (m)	2.2	Primary suspension damping (N*s/m)	6.00e4
Distance between axles (m)	12.6	Secondary suspension stiffness (N/m)	3.00e5
Length of train body (m)	19.0	Secondary suspension damping (N*s/m)	6.00e4
		Secondary suspension Bending stiffness (Nm/rad)	1.7e3

Due to the large size of the model, the wheel-rail contact is simplified as the contact between a node and beam, wherein the linear the Hertzian spring is applied.

The contact stiffness is calculated as Equation (1) [1].

$$k_H = \sqrt[3]{\frac{3E^2Q\sqrt{R_{wheel}R_{railprof}}}{2(1-v^2)^2}}, \quad (1)$$

where: E is the modulus of elasticity of the wheel and rail; v is the Poisson's ratio; Q is the static vertical wheel load; $\mathrm{R_{wheel}}$ is the radius of the wheel; $\mathrm{R_{railprof}}$ is the radius of the railhead [1].

The non-reflecting boundaries [55] are applied on both ends of the model to reduce the wave reflection. The bottom of the embankments (subgrade layer) and the bridge (concrete layer) are fixed.

The nonlinear connection between sleepers and ballast is crucial to model the degradation mechanism of ballast [20, 33]. In the real cases, sleepers generate a nonlinear interaction force to ballast under compression, and no force exists when they are hung [33] since sleepers and ballast are separable. Therefore, contact elements are applied between sleepers and ballast. According to the penalty algorithm employed in the contact elements, the search for penetrations between the bottom surface of sleepers and the top surface of ballast is made every time step during the calculation. When the penetration has been detected, a force proportional to the penetration depth is applied to resist and ultimately eliminate the penetration [34]. This method allows simulating the impact on ballast, which is proportional to the downward acceleration of sleepers.

This model inherently assumes that the stage 1 settlement has already completed and hence is mainly concerned with the stage 2 part of the transition zone settlement. It should be noted that the value of the initial settlement is important, but difficult to measure precisely in the real cases. For

instance, the void under sleepers measured in [56] had an error of 3mm. The value of the differential settlement used in the paper is selected from the values which were frequently reported in the field measurements in the transition zones [8, 9], ranged from 2mm to 10mm. The settlement in Stage 1 depends on axle loads and ballast condition. Higher axle loads and worse ballast condition lead to a higher settlement in Stage 1.In this study, 2mm is used since it can model the transition zone in good condition with a low axle load (14.5t). As a result, the predicted settlement is expected to be low. For higher values of the settlement in Stage 1, the prediction results should be higher. It is also remarkable to note that the model should be tuned according to field measurements before practical usage.

For convenience, the sleepers are numbered starting from the one closest to the bridge. They have the positive sign on the bridge-embankment transition and the negative sign on the embankment-bridge transition depending on the moving direction of the passing train. For example, the train passes Sleeper-10 to Sleeper-1 when it approaches the bridge, and later the train passes Sleeper+1 to Sleeper+10 when it leaves the bridge. Since the sleeper space is 0.6m, the distance from the bridge to each sleeper can be easily calculated. Note that there are no sleepers on the bridge.

At the equilibrium state of the model, due to the separable contact between sleepers and ballast, as well as the application of gravity and the resistance of rails, the voids between sleepers and ballast appear in the vicinity of the bridge, as shown in Figure 6.

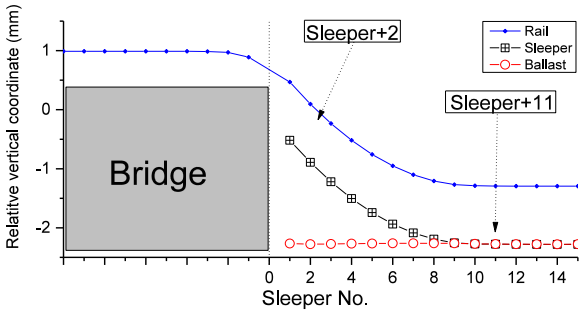

Figure 6: Vertical coordinates of rail, sleepers and ballast due to 2 mm settlement of ballast.

As shown in Figure 6, the first 10 sleepers close to the bridge are hung as a result of the initial settlement. After the Sleeper+11, the sleepers are fully supported by the ballast. Meanwhile, the hanging distance of Sleeper+1 is the highest, and the hanging distance gradually reduces as the distance from the bridge increases. From this figure, it can clearly be seen that the deflection line of the rail near the bridge is not linear. The hanging values of sleepers are presented as the difference between the vertical coordinates of sleepers and ballast. The same situation is observed on the other side of the bridge (in the embankment-bridge transition).

In the second phase of the simulation, the vehicle moves over the transition zone.

Figure **7** shows the time history of the vertical coordinates of two sleepers and the corresponding ballast elements, which are located close and far from the bridge (Sleeper+2 and Sleeper+11).

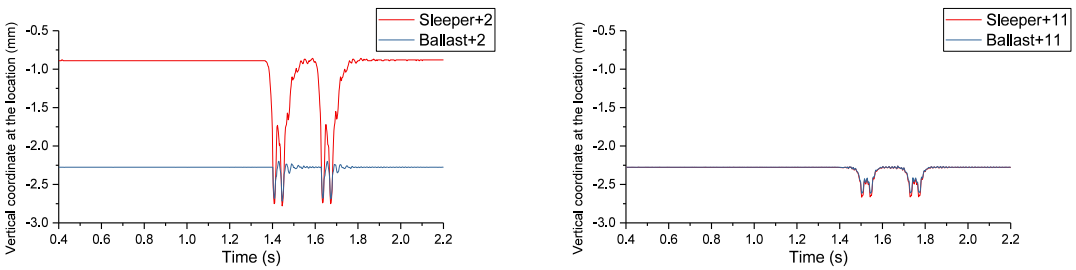

Figure 7: Time history of vertical coordinate due to the passing vehicle: sleeper +2 (left) and +11 (right).

As indicated in
Figure **7**, Sleeper+2 are hung before the train comes (1.6s). When the train moves above the sleeper during 1.6s to 2.4s, Sleeper+2 is pushed down and touches ballast, which also generates the displacements of ballast. After 2.4s, Sleeper+2 returns to its original hanging state, while Sleeper+11 is constantly rested on ballast. The significant distinction of the dynamic displacements of sleepers is a result of the differential settlement in the transition zone and may lead to the increase of wheel-rail contact forces and the increase of the stresses in ballast.

When sleepers contact ballast, the penetrations between the bottom surface of sleepers and the top surface of ballast occur. The stress distribution in ballast can be therefore calculated. Because the voids under sleepers are different depending on the locations (Figure 6), the stresses in the ballast elements under different sleepers also vary according to their locations (sleeper locations). An example of the stress distribution in ballast under Sleeper+2 corresponding to the four wheelsets is shown in Figure 8. The ballast elements under Sleeper+2 are considered as a group (unit), and the vertical stresses of the elements in the top later are collected as shown in Figure 8(a). The time history of the average stress under Sleeper+2 is shown in Figure 8(b), wherein the four peaks corresponding to the impacts of the four wheelsets during the train passage can be found. The closer two peaks belong to the two wheelsets of one bogie. The corresponding stress distributions at the four peaks are shown in Figure 8(c) to Figure 8(f).

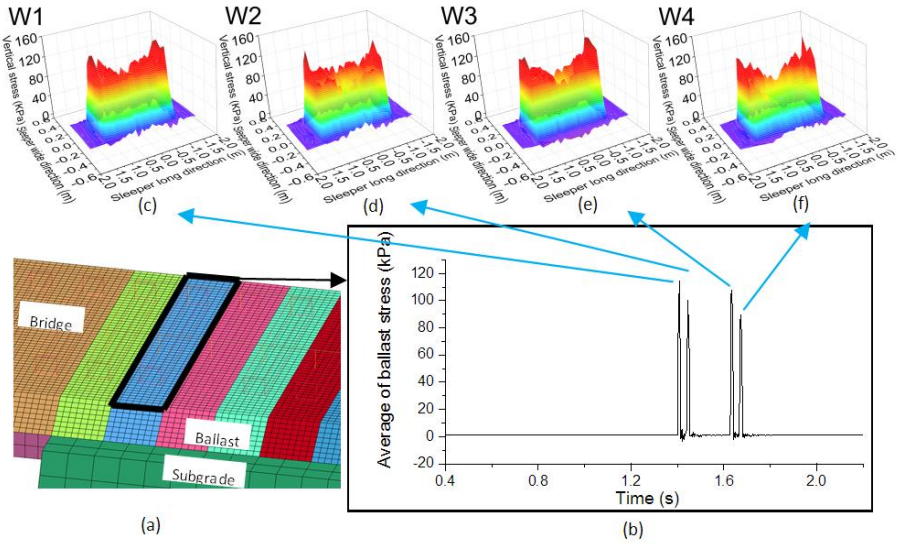

Figure 8: Stress distribution in ballast under Sleeper+2 from FE model.

As indicated in Figure 8, both the distribution and the average of the ballast stresses are different. The ballast stress generated by the second wheelset is higher than the stresses by other wheelsets. The obtained stresses can be used as the input to the settlement model, which is described in the next section. It should be noted that the FE model described above has been validated against the field measurements presented in [57, 58]. The comparison between the simulated rail displacements and the measured rail displacements in a transition zone is shown in Figure 9. The rail displacements were measured at multiple points in the transition zone during trains passing using a DIC-based device. The parameters of the model used in the simulation were adjusted according to the transition zone. More details of the validation can be found in [57, 58].

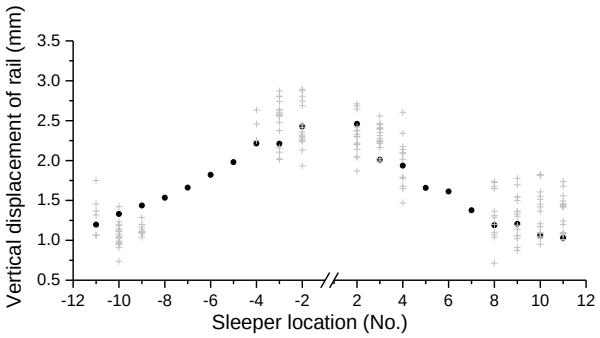

Figure 9: Comparison between measurements and simulation: black dots - simulation and cross - measurement results, from [57, 58].

3.2 Empirical settlement model

In this section, the empirical settlement model for ballast used in the methodology is introduced.

The total settlement of the ballast at location i can be calculated as:

$$S_i = S_{Ii} + S_{IIi}\ , \tag{2}$$

where S_i is the total settlement of the ballast at location i; S_{Ii} and S_{IIi} are the settlement of the ballast generated at location i in Stage 1 and Stage 2, respectively.

S_I is assumed to be 2mm as mentioned earlier, while S_{IIi} is a linear function of loading cycles, which can be written:

$$S_{IIi} = k_i \times N, \tag{3}$$

where k_i is the settlement rate at location i and N is the number of loading cycles.

The settlement rate k_i can be calculated by the widely used empirical settlement model for (open) ballast tracks, which describes the relationship between the settlement growth and the sleeper-ballast contact pressure. The empirical settlement model was initially proposed in [35] and later developed in [43]. According to this model, the key parameter influencing ballast settlement is the contact pressure between sleepers and ballast, which has been confirmed by the repeated loading experiments on sleepers. Similar conclusion can also be found in [20, 59, 60]. According to the settlement model in [35], the settlement growth is proportional to the sleeper-ballast pressure:

$$k_i = a{p_i}^n, \tag{4}$$

where p_i is the sleeper-ballast pressure (Pa) at location i; a and n are fitting coefficients.

A non-linear fit according to Equation (4) based on experimental data was first provided in [35], wherein:

$$k_i = 1.839 \times 10^{-13}{P_i}^4, \tag{5}$$

where P_i is the contact force between the sleeper and the ballast at location i. Later, a better fit was provided in [43], wherein it was found that the power $n = 5.276$ gives the best fit to the measured data, which reads:

$$k_i = 4.365 \times 10^{-12} \times {P_i}^{5.276}, \tag{6}$$

The two fitting curves are compared with the measurement data provided in [35], as shown in Figure 10.

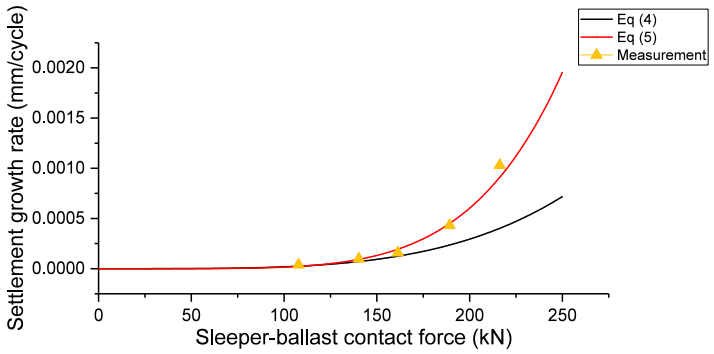

Figure 10: Two fitting curves compared from [35] and [43] with measurement data in [35].

As it can be seen from Figure 10, the curve provided in [43] fits better to the measurement data and it is therefore adopted in this study. Considering the contact area of the sleeper $A_{sleeper}$ is 0.68 m^2 (the nominal sleeper length 2570mm time the nominal sleeper width 265mm, as used in [49]), Equation (6) can be re-written as:

$$k_i = 4.365 \times 10^{-12} \times (0.68 \times p_i)^{5.276}, \quad (7)$$

The settlement rate k_i in Equation (7) is shown in Figure 11.

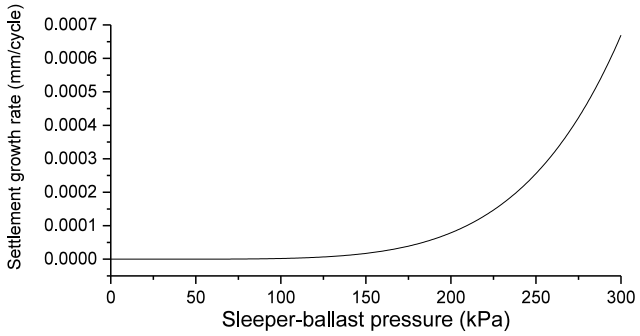

Figure 11: Relationship between the settlement growth and the sleeper-ballast pressure.

It can be seen from Equation (7) and Figure 11 that the settlement growth increases exponentially as the sleeper-ballast pressure increases. The loading at the lower level corresponds to the elastic behaviour of ballast, and therefore no settlement will occur. The settlement of the ballast grows in an elastic way until the sleeper-ballast pressure reaches around 135kPa. After that, there is a non-linear region where the settlement growth strongly depends on the sleeper–ballast pressure [43].

Using Equation (7) and assuming that the initial settlement $S_{Ii} = 2mm$, Equation (2) can be therefore rewritten as follows:

$$S_i = 2 + 4.365 \times 10^{-12} \times (0.68 \times p_i)^{5.276} \times N, \text{ (in mm)} \quad (8)$$

As indicated in Equation (8), the settlement of ballast S_i is a linear function of the loading cycle N, as p_i remains constant; and S_i is an exponential function of the sleeper–ballast pressure p_i, as N remains constant. Because the sleeper-ballast contact pressure varies to a large extent along the track in transition zones, the settlement at the different locations of transition zones will be different.

As mentioned previously, the ballast stresses at the location of each sleeper in transition zones can be calculated using the FE transition model. The sleeper-ballast pressure p_i is obtained from the FE model, which is equal to the average verical stress in the ballast under the i-th sleeper as described in Section 3.1. Using the average verical stress in the ballast as the input to Equation (8) instead of the sleeper–ballast pressure, the settlement after a certain loading cycle N can be obtained.

3.3 Integration of models

In this section, the iterative procedure for the prediction of the ballast settlement in transition zones is presented. The schematic diagram is shown in Figure 12. The prediction begins at Stage 2 of the settlement when the ballast track is settled uniformly with $S_{Ii} = 2mm$ (Figure 4(b)) after short time of operation due to the rapid compaction of ballast. The ballast stresses under each sleeper can be calculated using the FE model of transition zones, as it was described in Section 3.1. Then, using the ballast stresses as an input to the settlement model, the settlement under each sleeper after N loading cycles can be calculated according to Equation (8). Using these settlement values, the transition zone model can be updated, and the process will be iteratively repeated for the next N loading cycles. It should be noted that the ballast stiffness is assumed unchanged in the settling process.

Since the transition zone model is nonlinear by considering the sleeper-ballast contact, the settlement prediction after several iterations at location i is nonlinear. Therefore the prediction is affected by the iteration step N. The $N = 10{,}000\ cycles$ is adopted (in Section 4.1) to demonstrate the procedure, following [49]. Other values of the iteration step such as 5,000 cycles, 20,000 cycles, 30,000 cycles, and 60,000 cycles are also considered. The effect of the iteration step is discussed in Section 4.3.

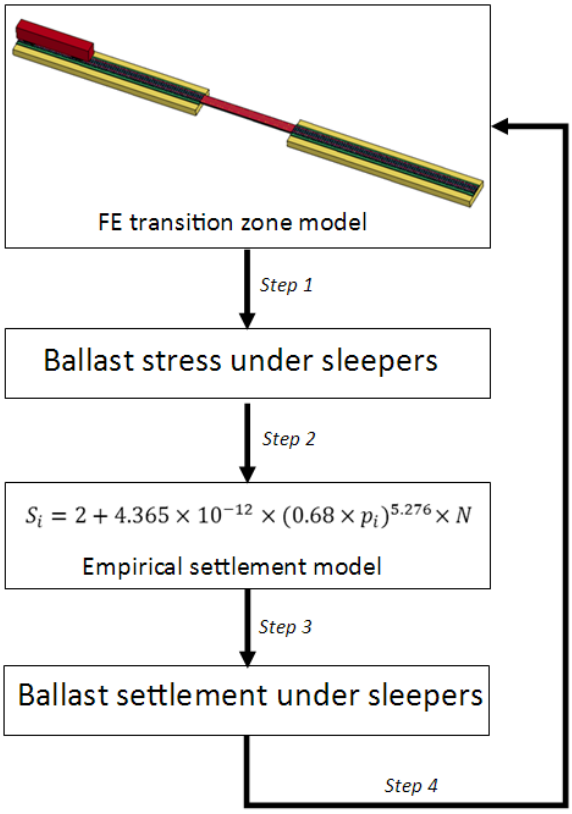

Figure 12: Iterative procedure to predict the settlement in track transition zones.

4 Numerical results

In this section, The iteration scheme is demonstrated by calculating the track settlement in the transition zone due to 60,000 loading cycles (3.5 MGT), when the transition zone is exposed to passenger trains. The dynamic responses such as the ballast stresses at 0 and 60,000 cycles (3.5 MGT)

are compared to study the effect of the settlement. The parametric study of the iteration step has been performed as well.

4.1 Numerical example

As mentioned earlier, the vertical stress in ballast at different locations along the track can be calculated using the FE model (see Figure 8). Since the permanent settlement of ballast is determined by the maximal stress in ballast [35, 61, 62], the maximum of the average ballast stress in the transition zone are collected, as shown in Figure 13.

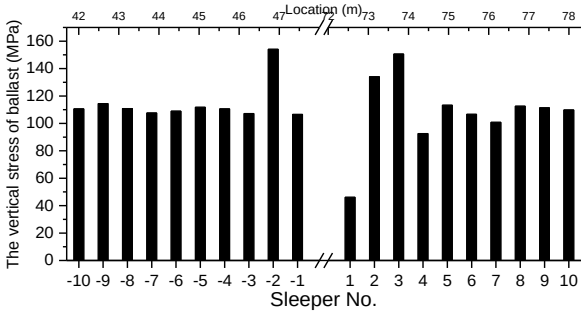

Figure 13: Ballast stress in the transition zone.

It can be seen from Figure 13 that the ballast closer to the bridge (under Sleeper-2, Sleeper +2 and Sleeper +3) suffers from higher stresses than the ballast in other locations. For example, the ballast stress under Sleeper -2 is almost 40% higher than that in other locations. The increase of the ballast stress is caused by the differential stiffness and settlement as well as the pitch motion of the vehicle [39].

Also, from Figure 13 it can be seen that the ballast stress in the embankment-bridge transition is different from that in the bridge-embankment transition. In the embankment-bridge transition the stress in ballast is relatively stable except Sleeper-2. In contrast, in the bridge-embankment transition, the stress in ballast fluctuates significantly. The wheels first drop off the bridge and impact on the ballast track (Sleeper+3); then, the wheels bounce over (Sleeper+4) and impact again on the ballast track (Sleeper+5) [39]. This "dropping" phenomenon is consistent with the theoretical analysis in [2].

Using the Equation (8) and the calculated ballast stress, the settlement of the transition zone after the first 10,000 cycles (corresponding to 2,000 train passages, assuming a train consisting of 5 vehicles) can be calculated, as shown in Figure 14.

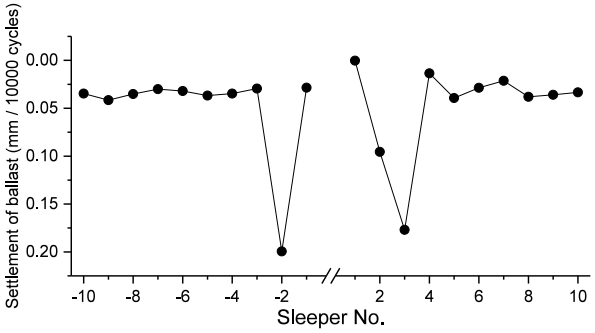

Figure 14: Prediction of the ballast settlement using the empirical settlement model.

It can be seen from Figure 14 that the settlement appears on both sides of the bridge, which may lead to two large deflections (dips) on each side of the bridge. For example, the ballast settlement under Sleeper-2 is 6 times higher than that in other locations in Figure 14, which explains the appearance of the extra settlement close to the bridge observed in [3, 6, 46]. It confirms the theory that the initial differential settlement caused by the rapid compaction of ballast (with different stiffness) leads to a geometry irregularity in transition zones.

By adding the calculated settlement values to the FE transition model, the ballast stresses under the new settlement condition can be calculated. After that, the settlement model can be used again to calculate the additional settlement based on the newly obtained stresses. Using this iterative procedure, the ballast settlement till 60,000 cycles (3.5 MGT) is predicted, as shown in Figure 15. Note that the iteration step N is 10,000 cycles and in total 6 iterations are performed.

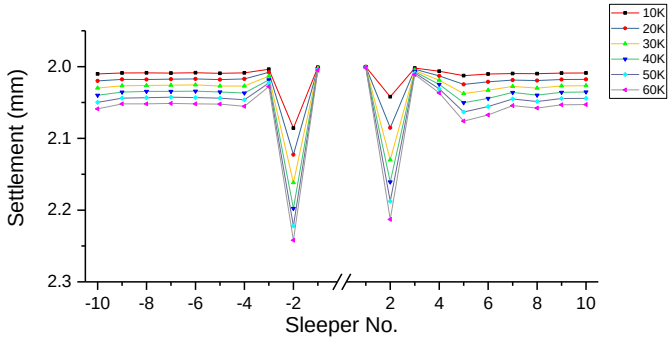

Figure 15: Prediction of track settlement in transition zone till 60,000 cycles (3.5 MGT).

Figure 15 clearly shows that the two dips continuously grow during the operation, which confirms the observation that once the dips appear, they keep growing instead of being self-healing. Hanging sleepers are expected in such locations.

It can also be found that the settlement in the embankment-bridge transition and the bridge-embankment transition is different. The ballast at Sleeper+5 settles with higher speed. This is also caused by the vibration of the vehicle, as discussed before. If the iterative calculation of the track settlement continues, the settlement at Sleeper+5 may exceed that at Sleeper+2.

It should be noted that the accumulated settlement is 0.24mm in the simulation, which is smaller than the settlement values often observed in the field. The reasons are that a high settlement is most probably caused by freight trains with higher axle loads, various axle loads in mixed traffic lines [63], and poor ballast condition. The model presented in the paper referred to a passenger train and good ballast condition (low settlement value in Stage 1 and “good” material property). In addition, the passage amount 60,000 (3.5 MGT) are relatively low.

The methodology for the settlement prediction in transition zones presented in this study can rather be used:

- for comparative analysis of various transition designs,
- for the qualitative study of the related phenomena (e.g. settlement shape in transition zones with different train movement directions),
- for the study of influential parameters (e.g. iteration step).

For these purposes, 60,000 cycles are sufficient, i.e. the trend can already be seen after that amount of cycles (the results for 100,000 cycles can be seen in Fig. 17). In addition, the calculations are very time-consuming since the model is in a large (120m) scale and the model considers the wheel-rail interaction and the sleeper-ballast interaction.

An example of the results using higher axle loads and higher passage amount can be found in [58]. It should be noted that the absolute value obtained using this methodology needs to be verified on the basis of measurement data, which is beyond the scope of this paper. Also, the settlement considered here does not include the subgrade settlement.

To have a better understanding of the trend of settlement and the settlement growth at different locations, the settlement at close locations (Sleeper-2 and Sleeper+2) are compared with the settlement at distant locations (Sleeper-8 and Sleeper+8) in Figure 16, as well as their growth.

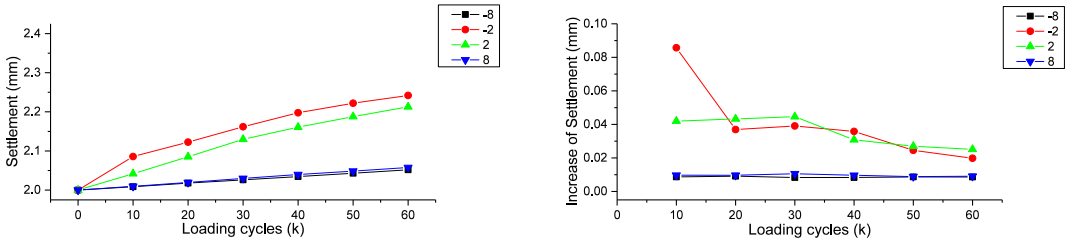

Figure 16: Settlement (a) and settlement growth (b) at the close locations (Sleeper-2 and Sleeper+2) and the distant locations (Sleeper-8 and Sleeper+8).

Figure 16 shows that the settlement growth of the ballast closer to the bridge (Sleeper-2 and Sleeper+2) is much higher, while the settlement growth of ballast at distant locations (Sleeper-8 and Sleeper+8) remains constant. The constant growth of the Sleeper-8 and Sleeper+8 confirms that the linear growth of the second stage of the settlement in the free ballast track, as in [41] (Stage 2 of the solid line in Figure 3). Moreover, the nonlinear settlement growth near the bridge (Sleeper-2 and Sleeper+2) confirms the suggested nonlinear settlement scheme (Stage 2) for transition zones (Stage 2 of the dashed line in Figure 3), which differs from the linear settlement scheme (Stage 2) for open tracks. By updating Figure 3 with the simulation results, the settlement scheme for transition zones can be obtained

It also proves that it is necessary to consider the non-linear contact between sleepers and ballast. By combining the settlement model for open tracks with the non-linear sleeper-ballast contact model (the FE transition model), the settlement in transition zones can be better predicted.

Furthermore, the settlement growth of ballast closer to the bridge is gradually reducing (Sleeper-2 and Sleeper+2 in Figure 16(b)). It implies that the amplified settlement growth at such locations may eventually decrease to the constant value as the ballast in distant locations. This is because the ballast pressure cannot increase infinitely due to the bending stiffness of rails. With the increase of loading cycles, the pressure will be distributed to neighbouring sleepers resulting in decreasing settlement growth rate [20]. However, since rails are fixed on the bridge side, the stress in rails will increase.

Considering the increasing growth of the settlement at Sleeper+5, it shows that once a dip (at Sleeper+2) is generated, the vertical growth of the dip reduces, while another dip appears at the adjacent location (Sleeper+5). It explains the fact that the ballast profile is very inhomogeneous, which is often observed in transition zones [50]. It also implies that when a track geometry irregularity is formed near the bridge, the geometry irregularity has a trend to spread further, since the differential settlement between bridges and ballast tracks cannot be eliminated.

4.2 Dynamic responses before and after the settlement

In this section, the dynamic responses of the FE model in transition zones before and after 60,000 cycles of passage (3.5 MGT) are compared. The purpose is to study the effects caused by the long-term settlement.

The comparison of the ballast stresses of 0 and 60,000 cycles of train passage (0 and 3.5 MGT) is shown in Figure 17. The collection method is the same as previously mentioned in Section 4.1.

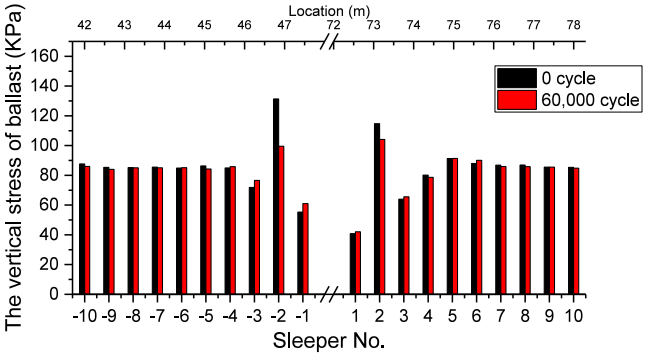

Figure 17: Comparison of ballast stress.

Figure 17 shows that the ballast stress is changed by the settlement, especially at Sleeper-2 and Sleeper +2. The stress in ballast after 60,000 cycles (3.5 MGT) is more evenly distributed along the track than in the beginning. The ballast stresses at Sleeper-2 and Sleeper +2 are reduced, from 131.3kPa to 99.5kPa and from 114.7kPa to 104.1kPa respectively. On the contrary, the ballast stresses at Sleeper-1 and Sleeper +1 are increased. The difference can be more clearly seen by comparing the variance of the ballast stresses in the embankment-bridge transition and the bridge-embankment transition, which is calculated after each iteration as shown in Figure 18.

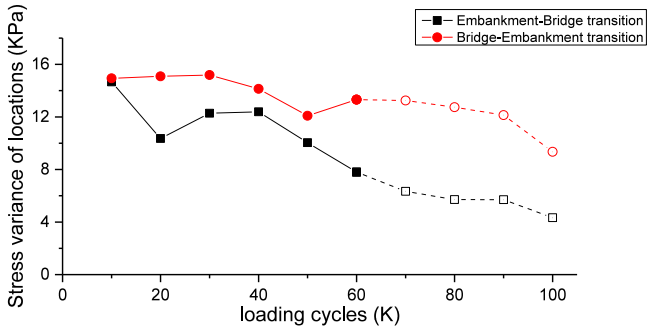

Figure 18: Variance of ballast stresses.

As indicated in Figure 18, the variance of the ballast stresses reduces gradually, which indicates that the ballast stress becomes evenly distributed as the number of loading cycles increases. This also indicates the growth of the dips will slow down. Note that even though the variance of ballast stresses in the bridge-embankment transition is increased at 60,000 loading cycles, it drops in the further iterations (from 60,000 cycles to 100,000 cycles), as shown in the dash lines in Figure 18. Compared with the bridge-embankment transition, the variance of the ballast stress in the embankment-bridge transition is reduced faster.

4.3 Parametric study of iteration steps

To study the influence of iteration steps, five values of the step are used to calculate the settlement of the transition zone till 60,000 cycles (3.5 MGT), or 12,000 train passages assuming 1

train including 5 vehicles. The values of the iteration step and the corresponding number of iterations to reach 60,000 cycles (3.5 MGT) are listed in Table 4.

Table 4: Iteration steps and number of iterations

Iteration step	Number of iterations
5,000 cycles/ 1,000 train passages	12
10,000 cycles/ 2,000 train passages	6
20,000 cycles/ 4,000 train passages	3
30,000 cycles/ 6,000 train passages	2
60,000 cycles/ 12,000 train passages	1

The settlements at 60,000 cycles (3.5 MGT) calculated by the five cases are shown in Figure 19. The settlement from 0 to 60,000 cycles (3.5 MGT) at the locations near the bridge (Sleeper-2 and Sleeper+2) and at distant locations (Sleeper-8 and Sleeper+8) are shown in Figure 20. The settlement of Sleeper-2 and Sleeper+2 at 60,000 cycles shown in Figure 20(a) and Figure 20(b) are listed and analysed in Table 5.

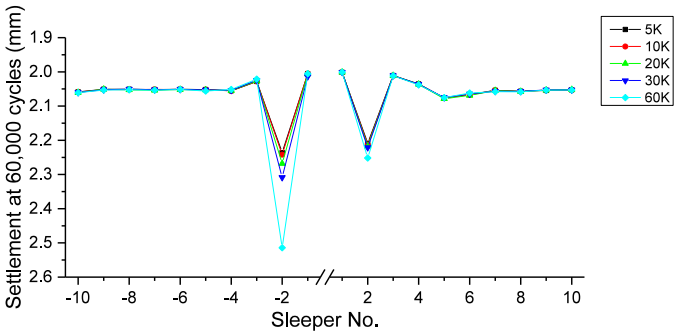

Figure 19: Settlement at 60,000 cycles (3.5 MGT) calculated different iteration step.

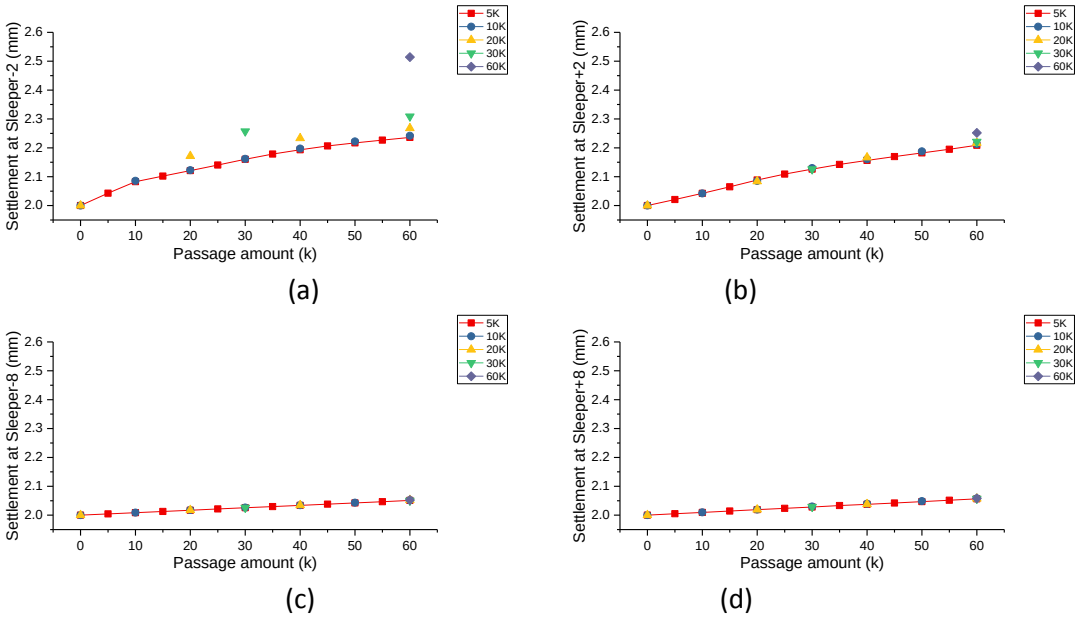

Figure 20: Settlement from 0 to 60,000 cycles (0 and 3.5 MGT) calculated different iteration step at close locations (Sleeper-2 and Sleeper+2) and distant locations (Sleeper-8 and Sleeper+8).

Table 5: Net settlement after 60,000 cycles (3.5 MGT) calculated by different steps

	Sleeper-2	Sleeper+2

Iteration step	Value (mm)	Increase percentage (%)	Value (mm)	Increase percentage (%)
5,000	0.236	-	0.209	-
10,000	0.242	2.5	0.213	1.9
20,000	0.268	13.6	0.217	3.9
30,000	0.309	30.8	0.221	5.9
60,000	0.514	117.8	0.252	20.6

As seen from Figure 19, Figure 20 and Table 5, the settlement prediction is affected by iteration steps, especially at dips, comparing the settlement at Sleeper-2 calculated by 60,000 cycles to 5,000 cycles, which is increased by 117.8%. On the contrary, the settlements at distant locations are almost unaffected.

Comparing the settlement at Sleeper-2 and Sleeper+2 calculated by different iteration steps, it can be found that the calculated results are increased as iteration steps increasing. To balance the calculation expense and error, the iteration step of 10,000 cycles is recommended.

5 Conclusions

To predict the permanent settlement of track transition zones, a methodology based on the FE model and the empirical settlement model has been presented. The FE model is a 3-D dynamic model (explicit integration) of a track transition zone modelled according to a widely used transition zone in the Netherlands. The transition model includes the nonlinear contact between sleepers and ballast as well as the vehicle dynamics. The empirical settlement model considers two stages of ballast settlement. The settlement in Stage 1 is expressed as a given value since it appears fast after operation due to the rapid compaction of ballast. The settlement in Stage 2 considers the nonlinear relationship between ballast stress and settlement. The iterative procedure includes the following steps. Firstly, the ballast stress due to passing trains under each sleeper is calculated using the FE model, after the ballast track is settled evenly after Stage 1. Then, the settlement is calculated using the empirical settlement model based on the ballast stresses obtained from the FE model. After that, by applying the obtained settlement to the FE model and performing the FE simulation again, the ballast stresses for the new settlement condition are calculated. The procedure continues iteratively until the requested number of cycles has been achieved.

To demonstrate the methodology, the ballast settlement in the transition zone after 60,000 loading cycles (3.5 MGT) is predicted. It has been shown that the settlements appear on both sides of the bridge already after the first 10,000 loading cycles. The two dips continuously grow as the number of loading cycles increasing, which confirms the track settlement often observed in transition zones.

The settlement growth varies depending on locations. The settlement growth of the ballast closer to the bridge is relatively high at the beginning (0 cycles) and then gradually reduced (during 60,000 cycles or 3.5 MGT). On the contrary, the settlement growth of ballast at distant locations remains constant. In addition, once a dip is generated, the vertical growth of the dip reduces, while another dip appears at an adjacent location along the track. This implies the track geometry irregularity will spread from bridges to the tracks on embankment.

By comparing the dynamic responses of the transition zone after 0 and 60,000 loading cycles (0 and 3.5 MGT), it has been found that the ballast stress after 60,000 cycles (3.5 MGT) is more evenly distributed. However, the stress in rails close to the bridge will increase.

The parametric study of iteration steps shows that the settlement prediction is strongly affected by iteration steps at the locations close to the bridge, while less affected at the distant locations. Moreover, the settlement predicted in the dip of embankment-bridge is increased as the iteration step increases. As a compromise between the expense and accuracy of calculations, the iteration step of 10,000 cycles is recommended.

Acknowledgement

The authors would like to thank ProRail, the Netherlands for providing the measurement data. The authors are very grateful to all the reviewers for their thorough reading of the manuscript and for their constructive comments.

References

1. Esveld C. *Modern railway track*. MRT-productions Zaltbommel, The Netherlands, 2001.
2. Kerr AD and Moroney BE. Track transition problems and remedies. *PROC OF THE AMERICAN RAILWAY ENGINEERING ASSOCIAT* 1993; 94: 25.
3. Li D and Davis D. Transition of Railroad Bridge Approaches. *JOURNAL OF GEOTECHNICAL AND GEOENVIRONMENTAL ENGINEERING* 2005. DOI: 10.1061//asce/1090-0241/2005/131:11/1392.
4. Plotkin D and Davis D. *Bridge approaches and track stiffness*. 2008.
5. Zuada Coelho B. *Dynamics of railway transition zones in soft soils (Doctoral dissertation)*. Doctoral dissertation, 2011.
6. Stark TD and Wilk ST. Root cause of differential movement at bridge transition zones. *Proceedings of the Institution of Mechanical Engineers, Part F: Journal of Rail and Rapid Transit* 2015. DOI: 10.1177/0954409715589620.
7. Nicks JE. *The bump at the end of the railway bridge (Doctoral dissertation)*. Texas A&M University, 2009.
8. Varandas JN, Hölscher P and Silva MAG. Dynamic behaviour of railway tracks on transitions zones. *Computers & Structures* 2011; 89: 1468-1479. DOI: 10.1016/j.compstruc.2011.02.013.
9. Hölscher P and Meijers P. *Literature study of knowledge and experience of transition zones*. 2007.
10. Hunt H. Settlement of railway track near bridge abutments. *Proceedings of the Institution of Civil Engineers-Transport*. Thomas Telford-ICE Virtual Library, 1997, p. 68-73.
11. Li Z and Wu T. Vehicle/track impact due to passing the transition between a floating slab and ballasted track. *Noise and Vibration Mitigation for Rail Transportation Systems*. Springer, 2008, pp.94-100.
12. Namura A and Suzuki T. Evaluation fo countermeasures against differential settlement at track transitions. *QR of RTRI* 2007; 48.
13. Lundqvist A, Larsson R and Dahlberg T. Influence of railway track stiffness variations on wheel/rail contact force. *Track for High-Speed Railways, Porto, Portugal* 2006.
14. Lei X and Zhang B. Influence of track stiffness distribution on vehicle and track interactions in track transition. *Proceedings of the Institution of Mechanical Engineers, Part F: Journal of Rail and Rapid Transit* 2010; 224: 592-604. DOI: 10.1243/09544097jrrt318.
15. Read D and Li D. Design of track transitions. *TCRP Research Results Digest 79* 2006. digest.
16. Sañudo R, Markine V and Dell'Olio L. Optimizing track transitions on high speed lines. *IAVSD2011* 2011.
17. Shahraki M, Warnakulasooriya C and Witt KJ. Numerical study of transition zone between ballasted and ballastless railway track. *Transportation Geotechnics* 2015; 3: 58-67. DOI: 10.1016/j.trgeo.2015.05.001.
18. Banimahd M and Woodward PK. 3-Dimensional Finite Element Modelling of Railway Transitions. *9th International Conference on Railway Engineering* 2007.
19. Banimahd M, Kennedy J, Medero GM, et al. Behaviour of train–track interaction in stiffness transitions. *Proceedings of the ICE - Transport* 2012; 165: 205-214. DOI: 10.1680/tran.10.00030.
20. Lundqvist A and Dahlberg T. Load impact on railway track due to unsupported sleepers. *Proceedings of the Institution of Mechanical Engineers, Part F: Journal of Rail and Rapid Transit* 2005; 219: 67-77. DOI: 10.1243/095440905x8790.

21. Gallego Giner I and López Pita A. Numerical simulation of embankment–structure transition design. *Proceedings of the Institution of Mechanical Engineers, Part F: Journal of Rail and Rapid Transit* 2009; 223: 331-343. DOI: 10.1243/09544097jrrt234.
22. Seara I and Correia AG. Performance assesment solutions for transition zones embankment-bridge railways trough numerical simulation 3D. *Semana de Engenharia 2010* 2010.
23. Shi J, Burrow MPN, Chan AH, et al. Measurements and simulation of the dynamic responses of a bridge-embankment transition zone below a heavy haul railway line. *Proceedings of the Institution of Mechanical Engineers, Part F: Journal of Rail and Rapid Transit* 2012; 227: 254-268. DOI: 10.1177/0954409712460979.
24. Paixao A, Fortunato E and Calcada R. Design and construction of backfills for railway track transition zones. *Proceedings of the Institution of Mechanical Engineers, Part F: Journal of Rail and Rapid Transit* 2013; 229: 58-70. DOI: 10.1177/0954409713499016.
25. Alves Ribeiro C, Paixão A, Fortunato E, et al. Under sleeper pads in transition zones at railway underpasses: numerical modelling and experimental validation. *Structure and Infrastructure Engineering* 2014; 11: 1432-1449. DOI: 10.1080/15732479.2014.970203.
26. Dahlberg T. Railway Track Stiffness Variations-Consequences and Countermeasures. *International Journal of Civil Engineering* 2010; 8.
27. Insa R, Salvador P, Inarejos J, et al. Analysis of the influence of under sleeper pads on the railway vehicle/track dynamic interaction in transition zones. *Proceedings of the Institution of Mechanical Engineers, Part F: Journal of Rail and Rapid Transit* 2011; 226: 409-420. DOI: 10.1177/0954409711430174.
28. Ling L, Dhanasekar M, Thambiratnam DP, et al. Minimising lateral impact derailment potential at level crossings through guard rails. *International Journal of Mechanical Sciences* 2016; 113: 49-60.
29. Ling L, Dhanasekar M, Thambiratnam DP, et al. Lateral impact derailment mechanisms, simulation and analysis. *International Journal of Impact Engineering* 2016; 94: 36-49.
30. Ling L, Dhanasekar M and Thambiratnam DP. Frontal collision of trains onto obliquely stuck road trucks at level crossings: Derailment mechanisms and simulation. *International Journal of Impact Engineering* 2017; 100: 154-165.
31. Ling L, Guan Q, Dhanasekar M, et al. Dynamic simulation of train–truck collision at level crossings. *Vehicle System Dynamics* 2017; 55: 1-22.
32. Sañudo R, dell'Olio L, Casado JA, et al. Track transitions in railways: A review. *Construction and Building Materials* 2016; 112: 140-157. DOI: 10.1016/j.conbuildmat.2016.02.084.
33. Varandas JN, Holscher P and Silva MA. Settlement of ballasted track under traffic loading: Application to transition zones. *Proceedings of the Institution of Mechanical Engineers, Part F: Journal of Rail and Rapid Transit* 2013; 228: 242-259. DOI: 10.1177/0954409712471610.
34. Hallquist JO. LS-DYNA theory manual. *Livermore software Technology corporation* 2006; 3: 25-31.
35. Sato Y. Optimization of track maintenance work on ballasted track. In: *Proceedings of the World Congress on Railway Research (WCRR'97), B* 1997, pp.405-411.
36. Wang H and Markine V. Analysis of the Long-Term Behaviour of Track Transition Zones. In: Pombo J, (ed.). *The Third International Conference on Railway Technology: Research, Development and Maintenance*. Civil-Comp Press, 2016, p. 203.
37. Lei X and Mao L. Dynamic response analyses of vehicle and track coupled system on track transition of conventional high speed railway. *Journal of Sound and Vibration* 2004; 271: 1133-1146. DOI: 10.1016/s0022-460x(03)00570-4.

38. Zhai WM and True H. Vehicle-track dynamics on a ramp and on the bridge: simulation and measurement. *Vehicle System Dynamics* 1999; 33: 11.
39. Wang H, Markine VL, Shevtsov IY, et al. Analysis of the Dynamic Behaviour of a Railway Track in Transition Zones With Differential Settlement. *2015 Joint Rail Conference, San Jose, California, USA, March 2015*. 2015, p. 7.
40. Gallage C, Dareeju B and Dhanasekar M. State-of-the-art : track degradation at bridge transitions. *Proceedings of the 4th International Conference on Structural Engineering and Construction Management 2013* 2013.
41. Sato Y. Japanese Studies on Deterioration of Ballasted Track. *Vehicle System Dynamics* 1995; 24: 197-208. DOI: 10.1080/00423119508969625.
42. Selig ET and Waters JM. *Track geotechnology and substructure management*. Thomas Telford, 1994.
43. Dahlberg T. Some railroad settlement models—a critical review. *Proceedings of the Institution of Mechanical Engineers, Part F: Journal of Rail and Rapid Transit* 2001; 215: 289-300. DOI: 10.1243/0954409011531585.
44. Indraratna B, Nimbalkar S, Christie D, et al. Field assessment of the performance of a ballasted rail track with and without geosynthetics. *Journal of Geotechnical and Geoenvironmental Engineering* 2010; 136: 907-917.
45. Suiker ASJ and de Borst R. A numerical model for the cyclic deterioration of railway tracks. *International Journal for Numerical Methods in Engineering* 2003; 57: 441-470. DOI: 10.1002/nme.683.
46. Varandas JN, Hölscher P and Silva MAG. A Settlement Model for Ballast at Transition Zones. *Proceedings of the Tenth International Conference on Computational Structures Technology* 2010.
47. Lichtberger B. Track maintenance strategies for ballasted track – a selection. *Rail Engineering International Edition* 2001.
48. Iwnicki SD, Grassie S and Kik W. Track Settlement prediction using computer simulation tools. *Vehicle System Dynamics* 2000; 33: 2-12.
49. Li X, Nielsen JCO and Pålsson BA. Simulation of track settlement in railway turnouts. *Vehicle System Dynamics* 2014; 52: 19. DOI: 10.1080/00423114.2014.904905.
50. Varandas JN. Long-Term Behaviour of Railway Transitions under Dynamic Loading Application to Soft Soil Sites (Doctoral dissertation). 2013.
51. Indraratna B, Thakur PK and Vinod JS. Experimental and Numerical Study of Railway Ballast Behavior under Cyclic Loading. *INTERNATIONAL JOURNAL OF GEOMECHANICS* 2010; 10: 136-144. DOI: 10.1061//ASCE/GM.1943-5622.0000055.
52. Fröhling RD. Low Frequency Dynamic Vehicle/Track Interaction: Modelling and Simulation. *Vehicle System Dynamics* 1998; 29: 30-46. DOI: 10.1080/00423119808969550.
53. Suzuki T, Ishida M, ABE K, et al. Measurement on Dynamic Behaviour of Track near Rail Joints and Prediction of Track Settlement. *QR of RTRI* 2005; 46: 124-129.
54. Holtzendorff K and Gerstberger U. Predicting Settlements of Ballasted Tracks due to Voided Sleepers. *Proceedings of the World Congress on Railway Research*. Koeln2001.
55. Hallquist JO. *LS-DYNA Keyword User's Manual*. LSTC Co., Livermore, CA, 2007.
56. Coelho Z. Dynamics of railway transition zones in soft soils. 2011. thesis.
57. Wang H and Markine V. Finite element analysis of the dynamic behaviour of track transition zones during train passing processes. *Submitted to Vehicle System Dynamics* 2017.
58. Wang H and Markine V. Analysis and improvement of the dynamic track behaviour in transition zone. In: al. Le, (ed.). *Tenth International Conference on the Bearing Capacity of Roads, Railways and Airfields*. Athens, Greece: Taylor & Francis Group, London, 2017.
59. Guerin N, Sab K, Moucheront P, et al. Experimental identification of a ballast settlement law. *CANADIAN GEOTECHNICAL JOURNAL* 1999; 36: 523-532.

60. Ionescu D, Indraratna B and Christie H. Behaviour of railway ballast under dynamic loads. *Proceedings of 13th Southeast Asian Geotechnical Conference, Taipei, Taiwan*. 1998, p. 69-74.
61. Stewart HE. Permanent strains from cyclic Variable-Amplitude loadings. *Journal of Geotechnical Engineering* 1986; 112: 646-660.
62. Iwnick S. Manchester Benchmarks for Rail Vehicle Simulation. *Vehicle System Dynamics* 1998; 30: 295-313. DOI: 10.1080/00423119808969454.
63. Kreiser D, Jia SX, Han JJ, et al. A nonlinear damage accumulation model for shakedown failure. *International Journal of Fatigue* 2007; 29: 1523-1530.